THE JOURNAL OF BIOLOGICAL CHEMISTRY
Vol. 280, No. 7, Issue of February 18, pp. 5527–5532, 2005
Printed in U.S.A.

Five Amino Acid Residues Responsible for the High Stability of *Hydrogenobacter thermophilus* Cytochrome c_{552}

RECIPROCAL MUTATION ANALYSIS*

Received for publication, November 2, 2004, and in revised form, December 6, 2004
Published, JBC Papers in Press, December 14, 2004, DOI 10.1074/jbc.M412392200

Kenta Oikawa‡, Shota Nakamura§, Takafumi Sonoyama‡, Atsushi Ohshima§, Yuji Kobayashi§, Shin-ichi J. Takayama¶, Yasuhiko Yamamoto¶, Susumu Uchiyama‖, Jun Hasegawa, and Yoshihiro Sambongi‡ ‡‡**

*From the ‡Graduate School of Biosphere Science, Hiroshima University, CREST of Japan Science and Technology Corp., 1-4-4 Kagamiyama, Higashi-Hiroshima, Hiroshima 739-8528, Japan, §Graduate School of Pharmaceutical Sciences, Osaka University, Suita 565-0871, Japan, ¶Department of Chemistry, University of Tsukuba, Tsukuba 305-8571, Japan, ‖Graduate School of Engineering, Osaka Univeristy, Suita 565-0871, Japan, and **Daiichi Pharmaceutical Co., Ltd., 1-16-13 Kita-Kasai, Edogawa-ku, Tokyo 134-8630, Japan*

Five amino acid residues responsible for extreme stability have been identified in cytochrome c_{552} (HT c_{552}) from a thermophilic bacterium, *Hydrogenobacter thermophilus*. The five residues, which are spatially distributed in three regions of HT c_{552}, were replaced with the corresponding residues in the homologous but less stable cytochrome c_{551} (PA c_{551}) from *Pseudomonas aeruginosa*. The quintuple HT c_{552} variant (A7F/M13V/Y34F/Y43E/I78V) showed the same stability against guanidine hydrochloride denaturation as that of PA c_{551}, suggesting that the five residues in HT c_{552} necessarily and sufficiently contribute to the overall stability. In the three HT c_{552} variants carrying mutations in each of the three regions, the Y34F/Y43E mutations resulted in the greatest destabilization, by −13.3 kJ mol^{-1}, followed by A7F/M13V (−3.3 kJ mol^{-1}) and then I78V (−1.5 kJ mol^{-1}). The order of destabilization in HT c_{552} was the same as that of stabilization in PA c_{551} with reverse mutations such as F34Y/E43Y, F7A/V13M, and V78I (13.4, 10.3, and 0.3 kJ mol^{-1}, respectively). The results of guanidine hydrochloride denaturation were consistent with those of thermal denaturation for the same variants. The present study established a method for reciprocal mutation analysis. The effects of side-chain contacts were experimentally evaluated by swapping the residues between the two homologous proteins that differ in stability. A comparative study of the two proteins was a useful tool for assessing the amino acid contribution to the overall stability.

Proteins from thermophilic bacteria usually exhibit enhanced stability against temperature or denaturants compared with the homologues from mesophiles (1, 2). Sequence comparison and rationally designed mutations of thermophilic and mesophilic proteins provide several lines of information on protein stability. In particular, investigation of the relationship between three-dimensional structure and thermodynamic parameters on protein unfolding provides detailed information on factors contributing to the stability.

A thermophilic hydrogen-oxidizing Gram-negative bacterium, *Hydrogenobacter thermophilus*, which grows optimally at 72 °C, produces a periplasmic Class I cytochrome c_{552} (HT c_{552})[1] (3). This bacterial cytochrome *c* has greatly contributed to the understanding of protein stability through pairwise comparison with homologous cytochrome c_{551} (PA c_{551}) from a mesophilic bacterium, *Pseudomonas aeruginosa,* which grows at 37 °C (4). These two proteins exhibit 56% sequence identity and have almost the same backbone conformations, but HT c_{552} is much more stable than PA c_{551} (5–9).

On precise structural comparison between HT c_{552} and PA c_{551}, we predicted that five amino acid residues spatially located in three regions were responsible for the higher stability of HT c_{552} (6). These residues were then introduced at the corresponding positions in PA c_{551} (7–9). The single mutation Val-78 to Ile (V78I) and two double mutations Phe-7 to Ala/Val-13 to Met (F7A/V13M) and Phe-34 to Tyr/Glu-43 to Tyr (F34Y/E43Y) in the corresponding three regions of PA c_{551} resulted in enhanced protein stability in an additive manner. Although the five residues were proved to be effective for stability, *e.g.* the denaturation temperature was elevated by more than 30 °C when they were introduced into the PA c_{551}, their roles in the original HT c_{552} remain unknown.

For an understanding of the high stability of HT c_{552}, the protein should be subjected to mutagenesis study. In this context, the HT c_{552} gene was first expressed as a modified holoprotein that had a covalently attached heme group in the cytoplasm of *Escherichia coli* or *Paracoccus denitrificans* with the attachment of an N-terminal Met residue (10, 11). Subsequently, the HT c_{552} apoprotein was targeted to the periplasm of *P. aeruginosa*, in which the protein became a holoprotein with the same spectral property as that of the authentic protein (12). Recently, HT c_{552} was expressed in the *E. coli* periplasm as a holoprotein with the aid of a cellular apparatus for cytochrome *c* maturation (*ccm* gene products) (13).

Here we established a new HT c_{552} expression system involving *E. coli* as a host and optimized the production level, which in turn facilitated further biophysical analyses of this protein.

* This work was supported in part by grants from Hiroshima University, the Noda Institute for Scientific Research, and the Japanese Ministry of Education, Science and Culture (grants-in-aid for Scientific Research on Priority Areas). The costs of publication of this article were defrayed in part by the payment of page charges. This article must therefore be hereby marked "*advertisement*" in accordance with 18 U.S.C. Section 1734 solely to indicate this fact.

‡‡ To whom correspondence should be addressed: Graduate School of Biosphere Science, Hiroshima University, 1-4-4 Kagamiyama, Higashi-Hiroshima, Hiroshima 739-8528, Japan. Tel. and Fax: 81-82-424-7924; E-mail: sambongi@hiroshima-u.ac.jp.

[1] The abbreviations used are: HT c_{552}, *H. thermophilus* cytochrome c_{552}; PA c_{551}, *P. aeruginosa* cytochrome c_{551}; GdnHCl, guanidine hydrochloride.

Amino acid residues were systematically substituted in the three regions of HT c_{552} with the corresponding residues of the less stable PA c_{551}. The thermodynamic parameters upon unfolding of the variants were compared with those of the reverse variants of PA c_{551}.

EXPERIMENTAL PROCEDURES

Bacterial Strains and Plasmids—*E. coli* DH5α was used to maintain plasmids. *E. coli* JCB387 was the host for testing the overexpression of HT c_{552} and its variants (11). The gene coding the mature HT c_{552} had been previously fused with the gene for signal sequence of PA c_{551} in the 5′ region (12), which was then inserted into the pKK223–3 vector (ampicillin resistance) under the control of the *tac* promoter. The resulting plasmid was designated as pKO2 and carried the wild-type HT c_{552} gene fused with the PA c_{551} signal sequence. Mutations A7F/M13V, Y34F/Y43E, I78V, and A7F/M13V/Y34F/Y43E/I78V (quintuple) were introduced into the fusion gene by a PCR-based method as described previously (7). For clarity throughout this paper the residues numbers used are those in PA c_{551}. The resulting mutated HT c_{552} genes with the PA c_{551} signal sequence were inserted into the pKK223–3 vector. Plasmid pEC86 (chloramphenicol resistance) carrying the *ccmABCDEFGH* genes for cytochrome *c* maturation proteins (14) was co-transformed into *E. coli* JCB387 together with pKO2 or its derivatives carrying the mutated genes.

Growth Conditions and Preparation of Periplasmic Protein Fractions—*E. coli* cells containing both pEC86 and pKO2 or their derivatives were initially grown in liquid LB medium containing 100 μg ml^{-1} ampicillin and 34 μg ml^{-1} chloramphenicol. The resulting cultures (1 ml) were inoculated into 100 ml of minimal medium containing 0.4% glycerol as a carbon source and the two antibiotics in 500-ml flasks, which were then shaken aerobically at 37 °C for an appropriate period before harvesting.

Periplasmic protein fractions of the *E. coli* cells were obtained by the cold osmotic shock method (15). The expressed HT c_{552} proteins in the periplasmic protein fractions were purified by HiTrap SP column chromatography (Amersham Biosciences), eluting with 25 mM sodium acetate buffer (pH 5.0) containing a NaCl concentration gradient (0–500 mM), followed by a Superdex 75 column equilibrated and eluted with 25 mM sodium acetate buffer (pH 5.0). The authentic HT c_{552} protein was also purified by the same method from *H. thermophilus* cells grown autotrophically as described (3). The protein purity was confirmed by SDS-polyacrylamide gel electrophoresis.

UV-Visible and NMR Spectroscopy and Cyclic Voltammetry of HT c_{552}—UV-visible spectra of HT c_{552} and its derivatives were measured with a Jasco 530 spectrophotometer. The NMR spectra of oxidized HT c_{552} at pH 7.2 and 25 °C were recorded on a Bruker Avance 600 FT NMR spectrometer operating at the ^{1}H frequency of 600 MHz. The protein concentration for the NMR analysis was ~1 mM in 90% H_2O 10% ^2H_2O. Chemical shifts are given in ppm downfield from sodium 2,2-dimethyl-2-silapentane-5-sulfonate with the residual H^2HO as an internal reference. Cyclic voltammetry assaying of HT c_{552} was carried out as described elsewhere (16). All potentials were referenced to the standard hydrogen electrode and calculated from the cyclic voltammogram as described.

Protein Denaturation—Thermal denaturation experiments involving circular dichroism (CD) were carried out in a newly developed pressure-proof cell compartment, which was attached to a Jasco J-720 CD spectrometer (17). This new apparatus facilitated thermal denaturation up to 180 °C. The oxidized proteins (20 μM) in HCl water (pH 5.0) were subjected to the following analyses. The temperature-dependent CD ellipticity change at 200–250 nm was followed in cuvettes of 1-mm path length. CD spectra were recorded from 40 to 160 °C with temperature intervals of 2–20 °C. The CD ellipticity changes at 222 nm were followed against temperature. Thermodynamic parameters were obtained using non-linear least-squares fitting with MATHEMATICA 3.0 as described previously (17).

Guanidine hydrochloride (GdnHCl) denaturation measurement by means of CD and nonlinear least-squares fitting of the data were performed according to the previous methods (7). HT c_{552} protein and its derivatives (20 μM) were incubated in diluted HCl water (pH 5.0) with varying concentrations of GdnHCl at 25 °C for 2 h before the measurements to equilibrate the proteins with the denaturant. The CD ellipticity at 222 nm of the protein solutions was measured at 25 °C. The oxidized proteins were used for measurement of denaturation as to both temperature and GdnHCl.

Other Procedures—The HT c_{552} contents in the periplasmic protein fractions were determined by measuring absorption spectra of solutions to which a few grains of solid sodium dithionite had been added. The extinction coefficient for reduced HT c_{552} at 552 nm, 20,400 M^{-1} cm^{-1}, was used to calculate the concentration of the cytochrome *c*. The N-terminal sequence of HT c_{552} expressed in the *E. coli* periplasm was determined with an automatic peptide sequencer (Hewlett Packard). Activity staining of SDS gels for covalently bound heme was also performed (18). The concentrations of the periplasmic protein fractions were estimated by the Bradford method using bovine serum albumin as a standard.

Materials—Restriction enzymes, Ex Taq polymerase, T4 DNA ligase, and other reagents for DNA handling were purchased from Takara Shuzou or Toyobo. GdnHCl (Ultra Pure) was purchased from ICN Biomedicals. All other chemicals used were of the highest grade commercially available.

RESULTS AND DISCUSSION

Expression of HT c_{552} in the E. coli Periplasm—The wild-type HT c_{552} protein expressed in the *E. coli* JCB387 strain was fully recovered in the periplasmic protein fraction after the cold osmotic shock but not in the membrane and cytoplasmic fractions. The expressed protein had a covalently attached heme, as judged on heme activity staining after separation by SDS-polyacrylamide gel electrophoresis (data not shown). The N-terminal amino acid sequence of the wild-type HT c_{552} protein expressed in the *E. coli* periplasm was determined to be Asn-Glu-Gln-Leu-Ala-Lys-Gln, which was identical to that of the authentic protein purified from the native organism, *H. thermophilus* (3). This indicates that the PA c_{551} signal peptide in the present fusion protein was correctly processed in the *E. coli* cells.

The time course of wild-type HT c_{552} production during aerobic *E. coli* growth was followed. The maximal production level (~25 mg liter^{-1} (culture)) was obtained several hours after the beginning of the stationary phase of cell growth. This high HT c_{552} production may be due to (i) the suitability of the PA c_{551} signal peptide that can target the apo-precursor protein efficiently to the *E. coli* periplasm, and (ii) the constitutive expression of *ccm* genes on the plasmid under aerobic conditions where the *E. coli* growth yield is higher than that under anaerobic ones (a natural control for the *ccm* genes). The efficient production and easy purification from the *E. coli* periplasm performed here enabled us to obtain a large amount of correctly processed HT c_{552}, which will facilitate further structural and mutagenesis studies.

Spectroscopic and Electrochemical Features of Heterologously Expressed Wild-type HT c_{552}—We next examined whether the heterologously expressed wild-type HT c_{552} exhibited the same spectroscopic and electrochemical properties as those of the authentic protein. The visible (400–600 nm) spectrum of dithionite-reduced wild-type HT c_{552} protein expressed in *E. coli* showed absorption maxima at 417, 521, and 552 nm, which are characteristic features of the authentic HT c_{552} protein (Fig. 1*A*). The far ultraviolet CD (200–250 nm) spectrum of the air-oxidized form of the expressed wild-type was also the same as that of the authentic protein, exhibiting CD ellipticity at 222 nm (Fig. 1*B*). The same properties in CD spectra were observed for all the variants examined in this study (data not shown), indicating that the variants did not markedly differ in terms of secondary structure.

Paramagnetically shifted signals arising from heme peripheral methyl and iron-coordinated methionine protons in ^{1}H NMR spectra were similarly observed for the oxidized forms of the expressed wild-type and authentic HT c_{552} (Fig. 2). These spectroscopic features suggested that His and Met residues are similarly coordinated to the heme iron in the expressed recombinant and authentic HT c_{552}. Thus, the expressed HT c_{552} polypeptide was correctly folded in the *E. coli* periplasm and did not differ in the spatial structure around the heme compared with that of the authentic protein.

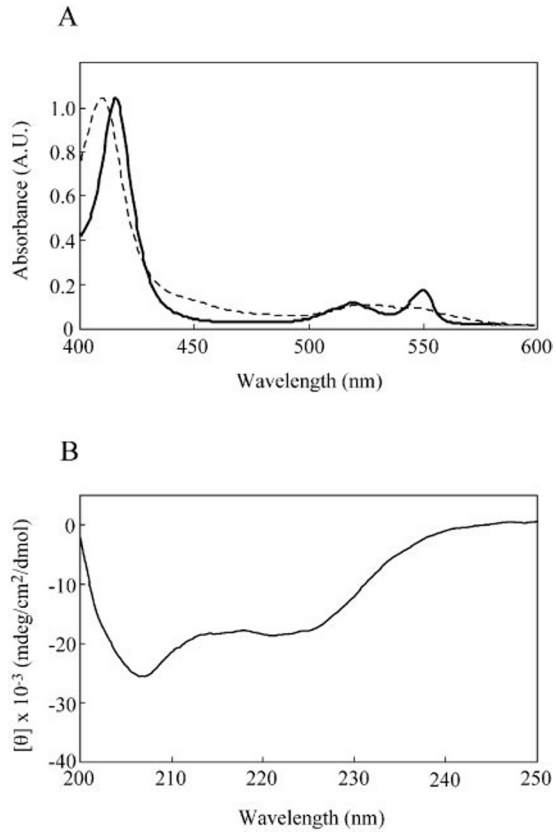

FIG. 1. **Visible and CD spectra.** *A*, visible spectra of dithionite reduced (*solid line*) and air-oxidized (*broken line*) forms of the wild-type recombinant HT c_{552} expressed in *E. coli* were measured at 25 °C and pH 5.0. *B*, CD spectra of the wild-type recombinant HT c_{552} were measured at 25 °C and pH 5.0.

To compare the redox properties of the expressed wild-type HT c_{552} and the authentic protein, we carried out electrochemical measurements using cyclic voltammogram. At 22 °C and pH 6.0, the redox potential ($E^{\circ\prime}$) value of the expressed protein was +250 mV, which was equivalent within error to that of the authentic value, +247 mV. Previously, we found that the $E^{\circ\prime}$ value of the authentic HT c_{552} exhibited a negative shift with increasing temperature up to 85 °C (16). This property was also conserved by the present heterologously expressed protein (data not shown).

Taken together, holo-HT c_{552} with a heme covalently attached, which in terms of spectroscopic and electrochemical features is indistinguishable from the native authentic protein, could be expressed in the periplasm of *E. coli*. Thus, using this expression system for thermophilic HT c_{552}, a site-directed mutagenesis study on the structural origin of its high stability can be performed as described below. The resulting thermodynamic data for HT c_{552} should be compared with those for a mesophilic counterpart PA c_{551}, that has been expressed in the *E. coli* periplasm with the aim of a mutagenesis study (7).

Destabilization of HT c_{552} as to GdnHCl Denaturation by Mutations—We first examined whether mutation(s) in HT c_{552} destabilized the structure as to GdnHCl denaturation. The mutated positions were 7, 13, 34, 43, and 78, where the original amino acid residues were replaced with the corresponding ones found in the less stable PA c_{551}. The mutated residues in HT c_{552} had been predicted to be responsible for the high stability from the results of three-dimensional structure analysis (6).

Fig. 3 shows GdnHCl-induced denaturation curves for HT c_{552} variants. The value for the midpoint of denaturation (C_m) of the variants (A7F/M13V, Y34F/Y43E, I78V, and A7F/M13V/Y34F/Y43E/I78V) became smaller as compared with that of the wild type (the difference in C_m between the wild-type HT c_{552} and variants (ΔC_m) were −0.76, −1.77, −0.48, and −2.78 M, respectively, Table I). The values for differences in the free energy change in water between the wild type and variants ($\Delta\Delta G^{\mathrm{W}}$) showed that the quintuple A7F/M13V/Y34F/Y43E/I78V variant had nearly the same stability as that of the mesophilic wild-type PA c_{551}. We have already shown that the quintuple reverse mutations in PA c_{551} (F7A/V13M/F34Y/E43Y/V78I) caused enhancement of stability to level in the wild-type HT c_{552} (8). These results together suggest that the five residues in HT c_{552} (Ala-7, Met-13, Tyr-34, Tyr-43, and Ile-78) necessarily and sufficiently contribute to the overall protein stability.

Correlation of Stability of the Reciprocal HT c_{552} and PA c_{551} Variants—Previously we obtained thermodynamic data for the GdnHCl denaturation of PA c_{551} variants having reverse mutations at positions 7, 13, 34, 43, and 78 (F7A/V13M, F34Y/E43Y, V78I, and F7A/V13M/F34Y/E43Y/V78I variants, Refs. 7–9). Because the experiments on these variants had been carried out under identical conditions (pH 5.0, 25 °C), we could compare the data with those obtained for the present HT c_{552} variants.

The differences in stability against GdnHCl denaturation ($\Delta\Delta G^{\mathrm{W}}$) between wild-type HT c_{552} and PA c_{551} and their reciprocal variants are shown in Fig. 4. In the three regional HT c_{552} variants (A7F/M13V, Y34F/Y43E, and I78V), the Y34F/Y43E mutations most strongly destabilized HT c_{552} as to GdnHCl denaturation ($\Delta\Delta G^{\mathrm{W}} = -13.3$ kJ mol^{-1}, Table I). Remarkably, the corresponding stabilizing effect of the reverse mutations (F34Y/E43Y) was prominent in the PA c_{551} variants under identical denaturation conditions (Fig. 4, Ref. 7). The difference in ΔG^{W} values between the wild-type PA c_{551} and F34Y/E43Y variant was 13.4 kJ mol^{-1} (7), *i.e.* close to the absolute value for $\Delta\Delta G^{\mathrm{W}}$ of the HT c_{552} Y34F/Y43E variant. This same contribution to the whole $\Delta\Delta G^{\mathrm{W}}$ value (ΔG^{W} difference between the values for two wild-type proteins) indicates that the effects of side chain interactions related to Tyr-34 and Tyr-43 are equal in the wild-type HT c_{552} and PA c_{551} F34Y/E43Y variant. Previous three-dimensional structure analysis of the wild-type HT c_{552} and PA c_{551} reverse quintuple variant showed that Tyr-34 and Tyr-43 contributes to the hydrophobic interaction and the formation of a hydrogen bond with one of the heme propionate side chains (6, 8). The present results indicate that the side chain interactions involving the two Tyr residues in the wild-type HT c_{552} and PA c_{551} F34Y/E43Y variant similarly contribute to the overall stability.

In contrast, the effect of A7F/M13V mutations on the overall stability of HT c_{552} ($\Delta\Delta G^{\mathrm{W}} = -3.3$ kJ mol^{-1}, Table I) was less than that of the corresponding reverse F7A/V13M mutations on the PA c_{551} stability ($\Delta\Delta G^{\mathrm{W}} = 10.3$ kJ mol^{-1}, calculated from Ref. 7) (Fig. 4). Three-dimensional structure analysis has indicated that Ala-7 and Met-13 in the wild-type HT c_{552} probably together cause tighter packing than that of the corresponding region of the wild-type PA c_{551} with Phe and Val residues (6). Other structure analysis showed that the PA c_{551} variant with the F7A/V13M mutations also caused tight packing, as found for the wild-type HT c_{552} (8). The same mutations in PA c_{551} change the Ile-18 side chain conformation to the thermodynamically favorable gauche plus form from the wild-type gauche minus form (as judged on $\chi 1$ dihedral angle analysis), which further results in tight packing in the same region of the PA c_{551} variant. From the results of these structure analyses, we have predicted that the region consisting of Ala-7 and Met-13 in the wild-type HT c_{552} and the PA c_{551} variant with the F7A/V13M mutations contributes to the high stability. The

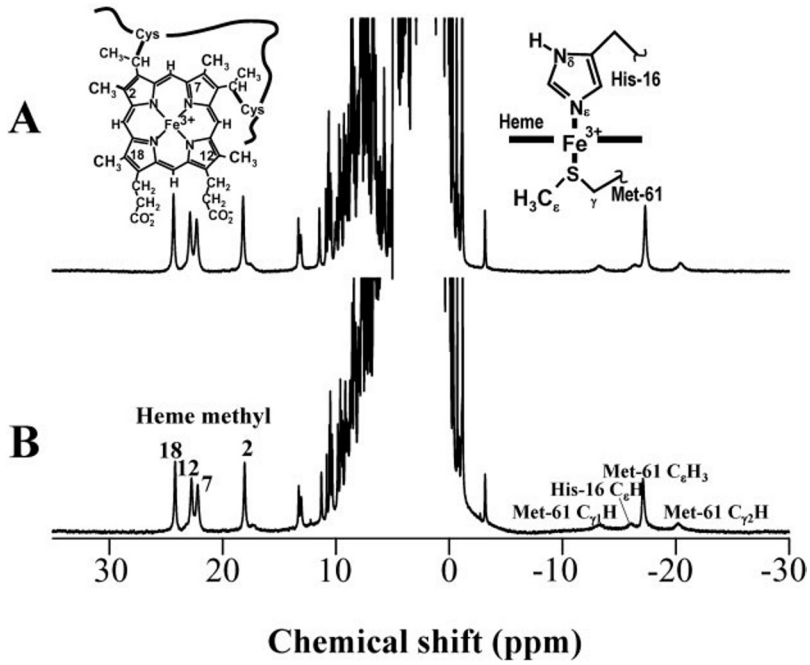

FIG. 2. **^{1}H NMR spectra.** Spectra for the wild-type recombinant HT c_{552} expressed in *E. coli* (*A*) and the authentic protein (*B*) are shown. The structures of the heme and axial ligands are illustrated in the *inset*. The assignments of some resolved signals are indicated in the spectra.

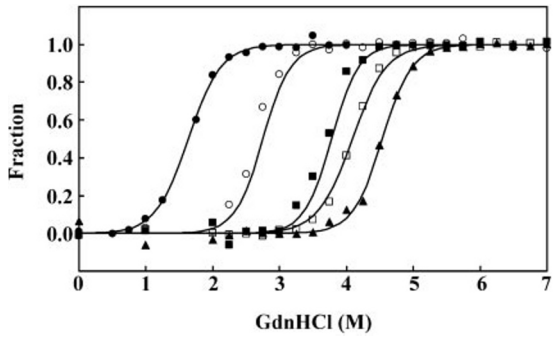

FIG. 3. **GdnHCl-induced denaturation.** Denaturation curves are shown as a function of GdnHCl concentration for the wild-type HT c_{552} (*closed triangle*), I78V (*open* square), A7F/M13V (*closed square*), Y34F/E43Y (*open circle*), and the quintuple variant (*closed circle*).

present less effective destabilization of the HT c_{552} protein caused by the A7F/M13V mutations indicates that, in contrast to in the case of the wild-type PA c_{551}, the side chains of the introduced Phe-7 and Val-13 still cause tight packing to some extent. In addition, the residue corresponding to PA c_{551} Ile-18 is Leu in HT c_{552}, whose side-chain conformation is presumably fixed as gauche plus form in both the wild-type and A7F/M13V variant because of steric hindrance between the isopropyl group and main-chain atoms. Thus, the effect of Leu-18 in HT c_{552} may not drastically differ regardless of the mutations at positions 7 and 13, as is the case for Ile-18 in PA c_{551}. Therefore, the effects of the A7F/M13V mutations in HT c_{552} are less than those of the reverse mutations in PA c_{551}.

Although we could not evaluate the effects of the I78V mutation in HT c_{552} and its PA c_{551} reverse mutation (V78I) precisely because of their smaller effects compared with the experimental error, the order of destabilization by the three HT c_{552} mutation(s) was the same as that of the stabilizing effects of reverse mutation(s) in PA c_{551}, as judged from the differences in ΔG^{W} values between the wild-type and variants (Fig. 4). In addition, the order of the ΔC_m values observed for HT c_{552} variants was the same as that for the increase in C_m reported for the reverse PA c_{551} variants (Table I, Ref. 7). In short, the more destabilizing mutation(s) in the three regions of HT c_{552} is the more effective mutation(s) in PA c_{551} when it is introduced in reverse.

Thermal Stability of HT c_{552}—We next measured the thermal stabilities of the wild-type HT c_{552} and its variants and then compared them with their stabilities against GdnHCl denaturation. HT c_{552} was so stable that we were not able to evaluate its thermodynamic property as to the pure effect of temperature using CD spectra (5, 8). Recently, however, we have newly developed a pressure-proof cell compartment that is attached to a CD spectrometer (17). The compartment can tolerate 10 atm, at which the boiling temperature of water is around 180 °C. Using this device, we could obtain complete thermal denaturation profiles for the highly stable HT c_{552} in both the oxidized and reduced states (17). This new system was used for thermal denaturation experiments on the oxidized forms of the wild-type HT c_{552} and its variants.

CD spectra (200–250 nm) of the proteins were measured from 40 to 150 °C at pH 5.0. The shapes of the spectra of all the proteins at the lower temperature did not differ significantly (see Fig. 1*B*, for an example). However, the CD ellipticities of the quintuple variant and the others began to change over 85 and 95 °C, respectively, as previously reported. The CD ellipticities at 222 nm were plotted against temperature, yielding thermal denaturation profiles of these proteins (Fig. 5). All the profiles exhibited complete single cooperation, indicating that the protein unfolding proceeded with a two-state transition.

From these CD measurements we obtained thermodynamic parameters for the thermal denaturation of HT c_{552} and its variants (Table I). The melting temperatures (T_m) of the wild-type, A7F/M13V, Y34F/Y43E, I78V, and the quintuple variants were 121.1, 117.0, 108.3, 117.8, and 95.2 °C, respectively. Differences in free energy changes between the proteins and the quintuple variant at the T_m of the quintuple variant ($\Delta\Delta G_m$) were calculated to quantify the stability against thermal denaturation. The resulting thermodynamic parameters showed that the quintuple mutation most decreased the overall stability followed by Y34F/Y43, A7F/M13V, and I78V ($\Delta\Delta G_m$ 9.8, 16.4, and 17.9 kJ mol^{-1}, respectively, compared with the quintuple variant).

Similarity and Difference in Stability against GdnHCl and Thermal Denaturation—Similar to the results of GdnHCl de-

TABLE I

Parameters characterizing the denaturation of HT c_{552} variants

From the GdnHCl denaturation profiles, the difference in free energy change between the folded and unfolded states (ΔG) was calculated as described by Pace (23). The free energy change in water (ΔG^W) and the dependence of ΔG on the GdnHCl concentration (m) were determined by least-squares fitting of the data for the transition region using the equation $\Delta G = \Delta G^W - m$[GdnHCl]. The midpoint of the GdnHCl denaturation (C_m) was the concentration of GdnHCl at which the ΔG value became zero. The differences in C_m (ΔC_m) and ΔG^W ($\Delta\Delta G^W$) between the wild type and variants were calculated by subtracting the values of the wild type from those of variants. The temperature of the midpoint of the transition (T_m) and the enthalpy change during denaturation at T_m (ΔH) were calculated from the basis of van't Hoff analysis. The entropy change during denaturation at T_m (ΔS) was calculated using the equation $\Delta S = \Delta H/T_m$. The differences in free energy changes of denaturation between the proteins and the quintuple variant at the T_m of the quintuple variant ($\Delta\Delta G_m$) were calculated using the equation given by Becktel and Schellman (24), $\Delta\Delta G_m = \Delta T_m \times \Delta S$ (quintuple variant), where ΔT_m is the difference in the T_m value between the proteins and the quintuple variant, and ΔS (quintuple variant) is the entropy change of the quintuple variant at the T_m.

Protein	C_m (ΔC_m)	ΔG^W ($\Delta\Delta G^W$)	T_m (ΔT_m)	$\Delta\Delta G_m$
	M	*kJ mol*$^{-1}$	*°C*	*kJ mol*$^{-1}$
Wild type	4.46 ± 0.18 (0)	44.9 ± 10.3 (0)	121.1 ± 1.0 (0)	19.5 ± 9.2
I78V	3.98 ± 0.18 (−0.48)	43.4 ± 8.2 (−1.5)	117.8 ± 0.6 (−3.3)	17.0 ± 3.3
A7F/M13V	3.70 ± 0.07 (−0.76)	41.6 ± 5.1 (−3.3)	117.0 ± 2.5 (−4.1)	16.4 ± 4.6
Y34F/Y43E	2.69 ± 0.05 (−1.77)	31.6 ± 1.3 (−13.3)	108.3 ± 1.2 (−12.8)	9.8 ± 2.1
Quintuple	1.67 ± 0.06 (−2.78)	20.0 ± 4.4 (−24.9)	95.2 ± 1.7 (−25.9)	0
PA c_{551}	2.25[a] (−2.21)	20.8[a] (−24.1)	86.4 ± 0.7[b] (−34.7)	−7.6 ± 2.2[b]

[a] Data are from Hasegawa *et al.* (7).

[b] T. Sonoyama and Y. Sambongi, unpublished data.

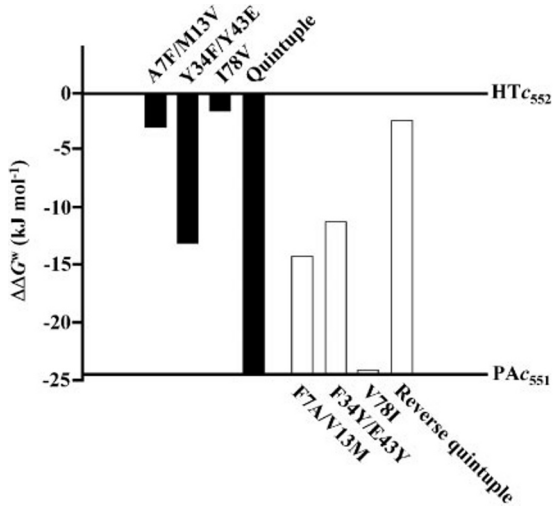

FIG. 4. **Effects of reciprocal mutations in HT c_{552} and PA c_{551}.** The experimental results of GdnHCl denaturation are shown. The relative stabilities of the parent proteins, HT c_{552} and PA c_{551}, are indicated by the *horizontal lines*. The first four entries are the relative differences in stability ($\Delta\Delta G^W$) caused by the substitutions of the respective residues of PA c_{551} in HT c_{552}. The *four bars* at the *right* show the stabilization of PA c_{551} by the reverse mutations.

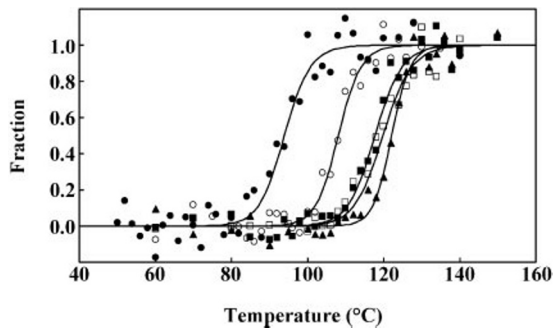

FIG. 5. **Thermal denaturation.** The unfolded fractions are plotted as a function of temperature. Denaturation curves are shown as for the wild-type HT c_{552} (*closed triangle*), I78V (*open square*), A7F/M13V (*closed square*), Y34F/E43Y (*open circle*), and the quintuple variant (*closed circle*).

naturation experiments, those as to the thermal denaturation showed that five residues, Ala-7, Met-13, Tyr-34, Tyr-43, and Ile-78, were responsible for the higher stability of HT c_{552}. In addition, the order of protein stability against GdnHCl denaturation (quintuple variant < Y34F/Y43E < A7F/M13V < I78V < wild type) was the same as that observed for thermal denaturation, as judged on the basis of the $\Delta\Delta G_m$ and T_m values (Table I). On the other hand, there is a difference in the effects of the two denaturation factors on the stability of the c_{552} quintuple variant. The variant showed almost the same stability as that of the wild-type PA c_{551} against GdnHCl denaturation, whereas the variant exhibited significantly higher stability than the PA c_{551} wild type against thermal denaturation, as manifested in the $\Delta\Delta G_m$ and T_m values (Table I).

Taken together, the present results indicated that the five mutations in HT c_{552}, leading to enhanced stability against GdnHCl denaturation, qualitatively resulted in elevated stability against temperature and vice versa. However, the reciprocal effect of the five mutations on the overall protein stability against thermal denaturation was not observed quantitatively. Further biophysical analysis of the HT c_{552} variants examined here and also the PA c_{551} reverse variants would help to explain the discrepancy between the two denaturation factors.

Other Mutations That Did Not Cause Destabilization of HT c_{552}—Do the five residues, Ala-7, Met-13, Tyr-34, Tyr-43, and Ile-78, exclusively determine the HT c_{552} stability? To address this question, we have already examined the effects of a few other mutations on HT c_{552} thermal stability in the presence of 1.5 M GdnHCl (19). GdnHCl should be added to obtain complete thermal-unfolding profiles of proteins below 100 °C on ordinary CD measurement. Using our former expression system in which the HT c_{552} protein is produced in the *E. coli* cytoplasm (10), we could transfer Lys, Ala, and Gly residues found in PA c_{551} to the corresponding positions of HT c_{552} (Ala-28, Lys-32, and Asp-39, respectively). Although all the proteins possessed a Met residue at the N terminus because the initial residue could not be cleaved off in the *E. coli* cytoplasm, we were able to evaluate the effects of mutations by comparison with the similarly expressed wild type. Three HT c_{552} variants with single mutations A28K, K32A, and D39G, and a double one, A28K/K32A, exhibited exactly the same stability as that of the wild type (12, 19). On the contrary, PA c_{551} variants carrying the A32K and G39D mutations exhibited the same stability as that of the wild-type protein, and the K28A mutation caused destabilization (19). Therefore, there is no reciprocal effect at positions 28, 32, and 39, which are located in α-helical regions and are exposed to the external solvent in both HT c_{552} and PA c_{551} (6). These observations in part substantiate the present finding that the five specific residues (Ala-7, Met-13, Tyr-34,

Tyr-43, and Ile-78) are among the limited and reciprocal determinants of the high stability of HT c_{552}.

Conclusion—In this study, we have established a HT c_{552} expression system involving *E. coli* as a host, with which we could produce 25 mg of HT c_{552} protein L (culture)$^{-1}$ in the periplasm. The expressed wild-type HT c_{552} exhibited the same physicochemical properties as those of the authentic one. This progress has facilitated mutagenesis study on HT c_{552} as to whether or not the specific amino acid residues reflect improvement in overall protein stability.

The present reciprocal mutation experiments involving HT c_{552} and PA c_{551} provided a unique opportunity to elucidate the protein stability in terms of the protein structure. We have shown previously that the five residues in HT c_{552} predicted to contribute to the overall protein stability were effective in enhancing the stability of PA c_{551} (7–9). The present study demonstrated that the reverse mutations of the selected five residues in HT c_{552} effectively destabilized the protein structure to the extent expected from the effects of the corresponding PA c_{551} mutations on the overall protein stability. In conjunction with the three-dimensional structure comparison, the effect of specific amino acid side chain interactions on the overall protein stability could be evaluated in both directions (stabilizing and destabilizing).

Perspectives—Finally, we should mention some limitations of the reciprocal mutation method, which will be useful for the development of general strategies for increasing protein stability through protein engineering. (i) A set of homologous proteins of interest should be small enough, each consisting of a single domain. Such proteins may have almost the same backbone conformation. (ii) Next, we should compare structural features to find interactions, such as side-chain packing, an ion pair, or a hydrogen bond, possibly responsible for the overall protein stability in a thermophilic protein. (iii) Reciprocal mutations should independently affect the overall protein stability. With the mutations, the backbone conformation should not change drastically so as not to affect other side chain interactions in remote regions.

The present results and another example of reciprocal mutation (20) more or less satisfy these criteria for methodological limitation. We can artificially control protein stability through the selection of amino acid residues contributing to the reciprocal stability. However, there is still a necessity to understand the general principle of protein stabilization, to study a strategy employed in an individual protein. Further accumulation of examples of reciprocal residue swapping between homologous native proteins together with artificially designed proteins (21, 22) will rationally reveal the principle of protein stability.

Acknowledgments—We thank Dr. L. Thöny-Meyer (Eidgenossische Technische Hochschule) for the kind gift of the pEC86 plasmid and Dr. K. Mizuta (Hiroshima University) for the helpful discussion.

REFERENCES

1. Jaenicke, R. & Bohm, G. (1998) *Curr. Opin. Struct. Biol.* **8,** 738–748
2. Jaenicke, R. (2000) *J. Biotechnol.* **79,** 193–203
3. Sanbongi, Y., Ishii, M., Igarashi, Y. & Kodama, T. (1989a) *J. Bacteriol.* **171,** 65–69
4. Sambongi, Y., Uchiyama, S., Kobayashi, Y., Igarashi, Y. & Hasegawa, J. (2002) *Eur. J. Biochem.* **269,** 3355–3361
5. Sanbongi, Y., Igarashi, Y. & Kodama, T. (1989b) *Biochemistry* **28,** 9574–9578
6. Hasegawa, J., Yoshida, T., Yamazaki, T., Sambongi, Y., Yu, Y., Igarashi, Y., Kodama, T., Yamazaki, K., Kyogoku, Y. & Kobayashi, Y. (1998) *Biochemistry* **37,** 9641–9649
7. Hasegawa, J., Shimahara, H., Mizutani, M., Uchiyama, S., Arai, H., Ishii, M., Kobayashi, Y., Ferguson, S. J., Sambongi, Y. & Igarashi, Y. (1999) *J. Biol. Chem.* **274,** 37533–37537
8. Hasegawa, J., Uchiyama, S., Tanimoto, Y., Mizutani, M., Kobayashi, Y., Sambongi, Y. & Igarashi, Y. (2000) *J. Biol. Chem.* **275,** 37824–37828
9. Uchiyama, S., Hasegawa, J., Tanimoto, Y., Moriguchi, H., Mizutani, M., Igarashi, Y., Sambongi, Y. & Kobayashi, Y. (2002) *Protein Eng.* **15,** 455–461
10. Sanbongi, Y., Yang, J-H., Igarashi, Y. & Kodama, T. (1991) *Eur. J. Biochem.* **198,** 7–12
11. Sambongi, Y. & Ferguson, S. J. (1994) *FEBS Lett.* **340,** 65–70
12. Zhang, Y., Arai, H., Sambongi, Y., Igarashi, Y. & Kodama, T. (1998) *J. Ferment. Bioeng.* **85,** 346–349
13. Karan, E. F., Russell, B. S. & Bren, K. L. (2002) *J. Biol. Inorg. Chem.* **7,** 260–272
14. Arslan, E., Schulz, H., Zufferey, R., Kunzler, P. & Thöny-Meyer, L. (1998) *Biochem. Biophys. Res. Commun.* **251,** 744–747
15. Sambongi, Y., Stoll, R. & Ferguson, S. J. (1996) *Mol. Microbiol.* **19,** 1193–1204
16. Terui, N., Tachiiri, N., Matsuo, H., Hasegawa, J., Uchiyama, S., Kobayashi, Y., Igarashi, Y. Sambongi, Y. & Yamamoto, Y. (2003) *J. Am. Chem. Soc.* **125,** 13650–13651
17. Uchiyama, S., Ohshima, A., Nakamura, S., Hasegawa, J., Terui, N., Takayama, S.J., Yamamoto, Y., Sambongi, Y. & Kobayashi, Y. (2004) *J. Am. Chem. Soc.* **126,** 14684–14685
18. Goodhew, C. F., Brown, K. R. & Pettigrew, G. W. (1986) *Biochim. Biophys. Acta* **852,** 288–294
19. Sambongi, Y. (1991) *Study on Thermal Stability of Cytochromes c.* Ph.D. thesis, University of Tokyo
20. Perl, D., Müller, U., Heinemann, U. & Schmid, F. X. (2000) *Nat. Struct. Biol.* **7,** 380–383
21. Kuroda, Y. & Kim, P. S. (2000) *J. Mol. Biol.* **298,** 493–501
22. Ishida, M., Dohmae, N., Shiro, Y., Oku, T., Iizuka, T. & Isogai, Y. (2004) *Biochemistry* **43,** 9823–9833
23. Pace, C. N. (1990) *Trends Biotechnol.* **8,** 93–98
24. Becktel, W. J. & Schellman, J. A. (1987) *Biopolymers* **26,** 1859–1877